Section I
Fundamentals

CHAPTER 1

Nanoscale Thermometry and Temperature Measurement

PETER R. N. CHILDS

Faculty of Engineering, Dyson School of Design Engineering, Imperial College London, Exhibition Road, London SW7 2AZ, UK
Email: p.childs@imperial.ac.uk

1.1 Introduction

Nanoscale temperature measurement concerns the determination of temperature or temperature difference at the sub-micron scale. Applications where it is important to be able to measure local temperature at the nanoscale include microelectronics, optics, microfluidics, chemical reaction and biochemical processes, such as living cells and nanomedicine. Examples of measurement of intracellular temperature fluctuations include ref. 1–13, microcircuit temperature mapping,[14–18] and microfluidics.[19–24] The topic of temperature measurement at the nanoscale has previously been reviewed.[25–27] The review by the author[28] provides a general overview of temperature measurement, along with the books in ref. 29 and 30. The long-standing series *Temperature its Measurement and Control in Science and Industry*[31–36] is also worth accessing for its archive on the topic.

In conventional temperature measurement a measurement system typically comprises a transducer to convert a temperature-dependent phenomenon into a signal that is a function of that temperature, a method to transmit the signal from the transducer, some form of signal processing, a display and method of recording the data. A calibration is then used to convert the measured quantity into a value of temperature and the significance of the

RSC Nanoscience & Nanotechnology No. 38
Thermometry at the Nanoscale: Techniques and Selected Applications
Edited by Luís Dias Carlos and Fernando Palacio

Published by the Royal Society of Chemistry, www.rsc.org

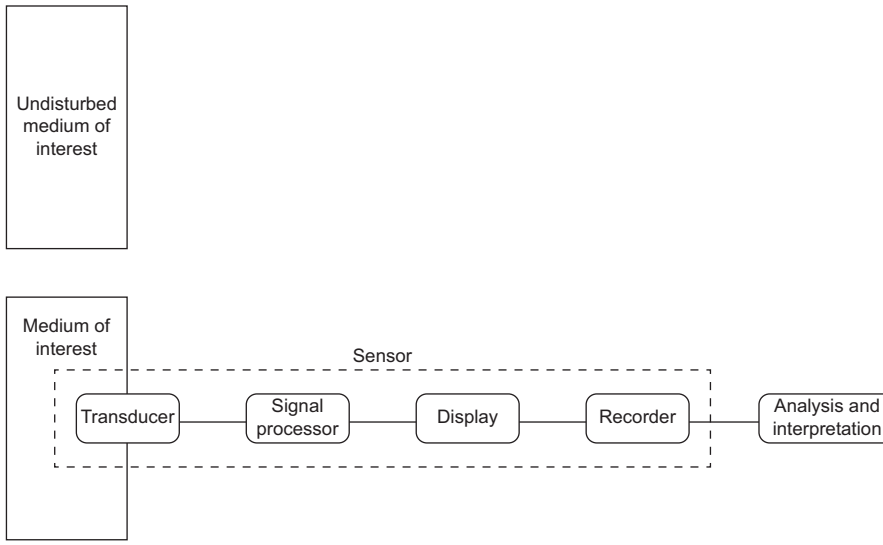

Figure 1.1 A comparison between the undisturbed medium and a typical temperature measurement application.

temperature can then be considered. Temperature measurement systems can be classified into broad themes, according to the physical contact between the transducer and the medium of interest, Figure 1.1, giving invasive, semi-invasive and non-invasive classifications.[28,29] Examples of each type respectively include thermocouples, thermochromic liquid crystals applied to a surface and observed remotely, and infrared pyrometry.

Miniaturisation of electronics and optoelectronics with higher switching speeds and associated energy dissipation has increased the importance of a good knowledge of localised heating in order to resolve manufacture and design issues and improve reliability. An accurate knowledge of living cell temperature is proving significant in monitoring cell health, with cancer cells, for example, exhibiting higher temperature than 'normal tissue' due to the increased metabolic activity.[5,7,8,37,38] Cell temperature alters with cellular activity such as division, gene expression and enzyme reaction, and temperature measurement at this scale can provide valuable diagnostic information.

Temperature can be regarded qualitatively as a measure of hotness or coldness of a body. Quantitatively temperature can be defined from the second law of thermodynamics in terms of the rate of change of entropy with energy.[29] Thermodynamically, temperature is the property that determines whether a system is in thermal equilibrium with another system or systems.

At the nanoscale, issues abound with the definition of temperature, as the scale of the applications means that assumptions of continuum and thermodynamic equilibrium may not hold.[39] For many practical applications, systems are in a non-equilibrium state and it is difficult to determine the conditions for which equilibrium is established at a local level.[40] A length

scale has been proposed[39] to identify whether a canonical energy distribution can be assumed. At very low temperatures, *e.g.*, 1 K, a length scale of 0.1 m was found for Si, providing an indication of the challenge for nanoscale measurements. However, the length scale necessary decreases as temperature rises, up to a limit, after which it is reasonably constant. For example a minimum length scale of 100 nm was identified for a temperature of 645 K. The implications of this for nanoscale temperature measurement remain significant, due to non-canonical energy distribution, non-equilibrium and ill-defined material properties. The definition of material properties is particularly important for some transient techniques where knowledge of specific heat capacity is necessary at the temperature of the body concerned.

In order to enable assignment of numerical values to bodies at different temperatures, a temperature scale is necessary. The thermodynamic temperature scale is defined by means of perfect heat engines. The SI unit for the thermodynamic temperature scale is the Kelvin. As perfect heat engines are not realisable in practice, the International Temperature Scale of 1990, denoted by ITS-90, has been developed as a practical approximation to the thermodynamic temperature scale. The ITS-90 is constructed using a number of overlapping temperature ranges and is believed to represent thermodynamic temperature to within ± 2 mK from 2 to 273 K, ± 3.5 mK at 730 K and ± 7 mK at 900 K (one standard deviation limits[41]). The ITS-90 enables traceability between the measurement that is actually made and the temperature scale defined by the ITS-90.

Due to the delicate and intricate nature of accurate measurements to ITS-90, most practical measurements are made using devices and systems that have been calibrated against another device which has itself been calibrated using guidelines specified in ITS-90. Calibration in this context is the process of relating the output value from a measurement system to a known input value. This process is illustrated in Figure 1.2 whereby there is a transfer of calibration between practical and specialist devices. The chain between the thermometer or temperature measurement system in use and

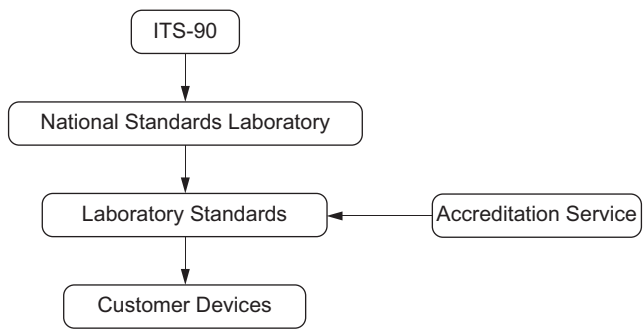

Figure 1.2 A typical chain between practical temperature measurement systems and the International Temperature Scale of 1990.

the ITS-90 may in practice have more links than those shown in Figure 1.2, with each link tending to increase the uncertainty associated with the measurement.

As well as the physical level of contact between a sensor and the application of interest, thermometric systems can be classified according to whether they are characterised by well-established equations of state that directly relate the measured parameter to temperature, and are known as *primary*, or if the system requires calibration then it is known as *secondary*. In addition, some materials exhibit an identifiable transition at a specific temperature, an example being phase change, and these can be useful for determining a particular temperature accurately, or to see if a temperature has been exceeded.[42]

1.2 Methods

A wide range of temperature measurement methods and technologies are available. Conventional technologies such as liquid-in-glass thermometry, thermocouples, and resistance temperature devices (RTDs), have all been adapted to nanoscale applications. Similarly, several of the remote observation approaches such as Raman, fluorescence and optical interferometry have been found to be useful for nanoscale applications The use of biological agents and cellular features to enable the measurement of temperature *in vivo* has provoked particular interest. Although a very wide range of temperatures is experienced in nature and science, here the technologies and temperature ranges considered are limited to those addressed by current technologies, which are generally applicable to cryogenic temperatures and the temperatures associated with electronic circuit operation. Temperature measurement methods relevant to the nanoscale include:

1. Liquid and solid-in-tube nanotube thermometry;
2. Resistance;
3. Thermocouples, based on the Seebeck effect;
4. Coulomb blockade;
5. MEMS (microelectromechanical systems) based resonator quality factor or Fermi-level shift;
6. Themochromic liquid crystals, based on crystal phase transitions;
7. Infrared thermography, based on Planck blackbody emission;
8. Fluorescence;
9. Thermoluminescence or thermographic phosphor thermometry;
10. Thermoreflectance, based on the temperature dependence of reflection;
11. Raman, based on inelastic scattering of monochromatic light;
12. Brownian motion;
13. Near-field scanning optical microscopy;
14. Scanning thermal microscopy, using an atomic force microscope with a thermocouple, thermistor or platinum resistance thermometer tip;

15. Transmission electron microscopy; and
16. Optical interferometry, based on thermal expansion or refractive index change.

In the context of nanoscale applications, the methods can be classified as *luminescent* or *non-luminescent*.[27] An overview of several of these methods is given in Sections 1.2.1 to 1.2.6. The presentation is inevitably brief, but is intended to introduce the principle, provoke interest and offer some relevant references. The chapters in this book also serve as excellent, more in-depth treatments.

1.2.1 Infrared

A body emits energy in the form of thermal radiation due to its temperature, with the quantity of radiation rising with increasing temperature. The energy emitted over the electromagnetic spectrum due to temperature by a black body can be modelled by Planck's law. Infrared thermometers measure the thermal radiation emitted by a body due to its temperature and conventional devices have found applications from cryogenic temperatures to over 6000 K. An infrared temperature measurement system generally consists of three elements, the emitting source of interest, the propagation medium, typically space or air, and the measuring device. An infrared measuring device may comprise an optical system, a detector, processing circuit, and display.[29,43] The purpose of the optical system is to focus the energy emitted by the target onto the infrared detector, typically converting the energy into an electrical signal. Infrared thermometers can be classified depending on whether the device is sensitive to all or a specific band of wavelengths, with those that are sensitive to all wavelengths classed as total radiation or broadband thermometers. Devices sensitive to radiation in a specific band of wavelengths are classed spectral band thermometers, ratio thermometers and thermal imagers. Infrared thermography represents a mature technology. For nanoscale applications the spatial resolution is limited, *ca.* 10 μm, and an estimate of the emissivity is necessary, at the temperature concerned. In addition, careful consideration needs to be given to reflection from other sources of thermal radiation in order to ensure that the measurement is close to the temperature of the undisturbed medium, or that appropriate compensation for this is made in the analysis.

1.2.2 Raman Scattering

Raman scattering refers to the inelastic scatting of light. When a molecule is promoted from the ground state to a higher state by incident radiation, it can either return to the original state, which is called *Rayleigh scattering*, or it can occupy a different vibrational state, which is classed as *Raman scattering*. Raman scattering gives rise to Stokes lines on the observed spectra.

Alternatively if a molecule is already in an excited state, it can be promoted to an even higher unstable state and then subsequently return to its ground state. This process is also called Raman scattering and gives rise to anti-Stokes lines on the observed spectra. Monitoring Raman scattering in order to determine temperature involves shining a monochromatic light source, such as a laser, on a sample and detecting the scattered light with a high-resolution Raman spectrometer. Fibre optics can be used for remote analysers. The process has the advantage that no preparation of the sample is necessary and small probe volumes, <1 μm, are possible. The method is time consuming and the numbers of samples per second is limited and can be as slow as 0.5 points per second. The application of Raman scattering thermometry has been applied to the polymerase chain reaction,[44] thermal transport in wires,[45,46] for strain temperature measurement, temperature and stress,[47] nanotubes,[48] nanowires,[49] and graphene.[50]

1.2.3 Luminescence

The thermal dependence of phosphor luminescence, band shape, peak energy, intensity, and excited states lifetimes can also be used for temperature measurement. The technique is also known as *thermographic phosphor thermometry*. A typical setup requires the phosphor or luminescent probe, applied and bonded to a surface, or incorporated within a medium, a light source such as a laser, and a detection system. Types of luminescent thermal probes include organic dyes, ruthenium complexes, quantum dots, Ln^{3+} ions, polymer and organic–inorganic hybrid matrices incorporating emitting centres. The method has the advantages of remote observation, high sensitivity, good spatial resolution and short acquisition periods.

1.2.3.1 Organic Complexes

Organic complexes are readily available and can be selected based on parameters such as the excitation/emission wavelength range required, solubility and facility of vectorisation. An example is nanoparticles of Ru(phen) and PtTFPP embedded in polyacrylonitrile.[51,52] Ru(phen) has a maximum temperature sensitivity of 2.5% K^{-1} at 320 K. Alternatively, a ratio of intensities from the monomer and excimer/exciplex can be analysed.[53] Similarly, the decay of emission lifetimes can be used.

1.2.3.2 Quantum Dots

Quantum dots (QDs) are nanocrystals of a semiconducting material with diameters in the range of about 2 to 10 nm. The high surface-to-volume ratios for these particles results in quantum mechanical properties, such as temperature-dependent photoluminescence, which can be exploited for the purpose of temperature measurement. An example is ZnS-coated CdS, which

gives a factor of five change in photoluminescence intensity over the range of 100 to 500 K.[54,55] The method involves observing the QDs through a microscope. A series of factors have limited the use of QDs for thermometry to date, including bluing, bleaching and blinking under continuous illumination.[56–58] To overcome some of the practical limitations QDs can be coated with an inert material. The development of a III-nitride QD embedded in a nanowire for room temperature applications has been reported by Holmes *et al.*[59] The design of QDs for *in vivo* applications has also been considered.[60]

1.2.3.3 Phosphors

The luminescent properties of thermographic phosphors are temperature dependent. This dependency can be observed by applying a thin layer of luminescent material to the system of interest, illumination with UV light and observing the subsequent luminescence. There are two commonly used response modes.[61,62] A pulsed excitation source can be used and after each pulse the phosphor exhibits an exponentially decaying emission, the time constant of which is temperature dependent. Alternatively, pulsed or continuous illumination can be used and the ratio of the emission intensities of two distinct spectral lines can be determined, which is temperature dependent.

Ln^{3+} can be incorporated into a polymer binder and sprayed onto a surface.[62] A measurement system will typically comprise the surface of interest, the applied coating, a means of exciting the phosphor, such as a laser, and an optical detector or photomultiplier. The use of the lanthanide coordination polymer $Tb_{0.957}Eu_{0.043}$cpda as a ratiometric and colorimetric luminescent thermometer for the temperature range 40 to 300 K has been reported.[63]

Thin film deposited chromium-doped aluminium oxide ($Cr–Al_2O_3$, ruby) thermographic phosphors for temperature measurement have been used.[64] Zinc silicate ($Zn_2SiO_4:Mn^{2+}$) has been shown to be highly suitable for fluorescence intensity ratio temperature measurement over the range of 30 to 300 °C with a sensitivity of 12.2%.[65] The detailed characteristics of fluorescence spectra measurements have been exploited,[66] in combination with a neural network analysis, in order to determine absolute temperature and this has been demonstrated for Rhodamine B (RhB) and copper chloride dyed glycerol. Polydiacetylene (PDA) embedded PVA film can be used to measure thermal gradients effectively.[67]

1.2.3.4 Biomolecular Intracellular Thermometers

A series of technologies and approaches have been taken to explore possibilities for measuring temperature at the cellular level. These range from the introduction of fluorescent probes and dyes, to the introduction of proteins to control gene expression, the use of materials for the controlled

release of chemicals sensitive to temperature, QDs, near-infrared imaging, and heating of nanoparticles to induce cell response at a known temperature. The use of temperature-sensitive green emission of fluorescent $NaYF_4$:Er^{3+},Yb^{3+} nanoparticles over the range 25 to 45 °C with application to HeLa cells has been demonstrated.[68] The use of RhB dye employed as a temperature indicator within a single cell has been reported[69] with a resolution of better than ± 0.3 °C within the cell cytoplasm, but this reduces to ± 1.8 °C as a result of environmental variations. Temperature-sensitive mutants of LacI controlling LacZ expression have been explored.[38] Great care is necessary with such approaches as the signal can be a function of duration at a temperature as well as the magnitude of the temperature. Mesoporous materials, such as silica nanoparticles, offer the potential for the controlled release of chemicals that are responsive to temperature changes and this concept has been explored.[70–72] The heating of nanoparticles of gold injected into a cell, in combination with optical detection of electron spin resonance in single atomic defects in nitrogen vacancy (NV) diamonds, as the sensor, has been demonstrated.[10]

An early example[2] of using luminescence intensity to measure cell temperature used the temperature-dependent luminescence intensity of the $Eu(tta)_3 \cdot 3H_2O$ complex.

A polymer-based thermometry solution has been demonstrated[5] using PNIPAM combined with the water-sensitive fluorophore, DBD-AA. They successfully measured temperatures within the cell over the range 300 to 306 K with a temperature resolution of 0.3 to 0.5 K and a sensitivity of $S_m = 94\%\ K^{-1}$ at 304 K.

Further consideration of the topic of cell-based temperature measurement is given in Section 1.2.6.4.

1.2.4 Thermoreflectance

Thermoreflectance exploits the temperature dependence of a material's refractive index, using an optical imaging system to observe the surface of interest, with the temperature profile resolution defined by the special resolution of the optical system.[14,26]

1.2.5 Interferometry

Optical interferometry provides both local temperature information, as well as local deformation due to thermal expansion. Interferometers measure differences in optical paths between two light beams, one of which bypasses the test section, while the other passes directly through the test section. A quadriwave lateral shearing interferometer as a wavefront sensor has been used[73] for determining the variation of refractive index for a microwire. Using a water layer on the microwire, and electrical heating, variations in the refractive index generate a distortion of the incident wavefront, enabling mapping of the temperature field.

1.2.6 Non-luminescent

A number of non-luminescent temperature measurement technologies have been developed for nanoscale applications including scanning thermal microscopy, nanolithography, carbon nanotubes, and biomaterials.

1.2.6.1 Scanning Thermal Microscopy

Scanning thermal microscopy uses a small thermocouple with a junction diameter of the order of 20 to 100 nm, formed at a probe tip which is traversed over the surface of interest.[74–76] Alternatively an RTD can be mounted on the probe or a combination of a thermocouple and RTD. This can be useful for determining the thermal conductivity of a sample.[77–79]

1.2.6.2 Nanolithography

Vapour deposition technology[80] can be used to deposit a platinum strip to form a sensor on a surface. Examples include decomposition of organic inks such as $(CH_3)_3Pt$. Combinations of materials can be built up by appropriate layering in order to ensure electrical isolation and lead-outs. US Patent 6905736[81] reports a Pt(Ga)–W(Ga) junction with a temperature coefficient of 5.4 $mV\,^{\circ}C^{-1}$. 100 nm^2 gold–nickel thermocouples on silicon and 500 nm^2 thermocouples on quartz have also been produced.[82] A challenge with vapour deposition sensors is ensuring robustness of the sensor, and chemical consistency. It is well known that some materials aggressively leach elements from a substrate, gradually degrading the performance of a sensor with time.

1.2.6.3 Carbon Nanotube Thermometry

Liquid-in-glass thermometry provided the basis for modern temperature measurement.[29,30] Carbon nanotube thermometry was originally proposed[83] using gallium as the thermometric liquid, with a scanning electron microscope to observe the meniscus. The coefficient of thermal expansion of gallium has been observed[83] to vary linearly over the range 323 to 773 K, with values close to the macroscopic quantities. Examples of other thermometric liquids proposed and demonstrated for different temperature ranges include Pb using a ZnO nanotube,[84] Au(Si) using a Ga_2O_3 nanotube,[85] and In using In_2O_3 nanotubes.[86] The use of carbon nanotubes to provide good thermal contact between a microscope and sample has also been reported.[87]

1.2.6.4 Biomolecular-Based Thermometry

Many molecules and biological components exhibit temperature-dependent behaviours that can be exploited for temperature measurement on the

nanoscale. Examples include the introduction of proteins to control gene expression, crystal defects, and luminescence.

As noted previously, temperature represents a fundamental parameter for the operation of living cells and a number of mechanisms are apparent that can be exploited or mimicked in the measurement or control of temperature.[88] For histidine kinase, DesK, from Bacillus subtilis, Albanesi *et al.*,[89] report how the plasticity of the helical domain influences the catalytic activities of the protein, through conformational signals transmitted by membrane connections enabling interhelical rearrangements, controlling the alternation between output autokinase and phosphatase activities. Of interest, Albanesi *et al.*[89] suggest that structural comparison of the different DesK variants indicates that incoming signals can take the form of helix rotations and asymmetric helical bends comparable to some other sensing systems, and that similar switching mechanisms could be operational in a wide range of sensor histidine kinases, or indeed exploited in newly designed mechanisms.

Crystal defects, notably the NV centre, in diamond can be exploited to enable the measurement of a series of physical parameters including temperature. The optical excitation of NV nanodiamonds with 532 nm laser light and fluorescence collection with a confocal microscope has been reported by Neumann *et al.*,[10] yielding a noise floor of 130 mK $Hz^{1/2}$ and accuracies as good as 1 mK. Embedded in nanocrystals they can provide robust single-photon sources and fluorescent biomarkers.[13] Nanodiamonds can be injected into a cell, and excited with a laser to alter their spin state and the light emitted measured. By using more than one nanodiamond the temperature difference within a single cell can be evaluated as reported by Kucsko *et al.*,[11] detecting temperature differences as small as 1.8 ± 0.3 mK. Interestingly Kucsko *et al.*[11] report that by combining nanodiamonds with laser heating of gold particles also injected into a cell, the temperature of the cell can be controlled.

Living cells sense temperature through proteins, nucleic acids and mRNAs that either modify their conformation structure directly[90–92] or undergo complex reactions. Cells respond to harmful temperature changes by inducing heat-shock or cold-shock proteins. RNA temperature-sensing capability is located in specific areas of RNA structure, especially the 5′ untranslated region of certain heat-shock and virulence genes, which shields the ribosome-binding sites at physiological temperatures.[93] Under the onset of heat-shock, destabilisation of RNA commences with associated release of ribosome-binding sites and translation initiation. For cold-shock, cell growth tends to stop, accompanied by a dramatic reduction in bulk gene expression and cold-shock proteins are expressed. The underlying mechanism in cells involves a gradual melting of a weak stem-loop structure rather than a switch between two mutually exclusive conformations. As such, RNA thermometers can be considered as *molecular dimmers* rather than discrete on and off state switches.[93] Naturally occurring thermometers represent highly complex systems, but simpler RNA stem-loop structures,

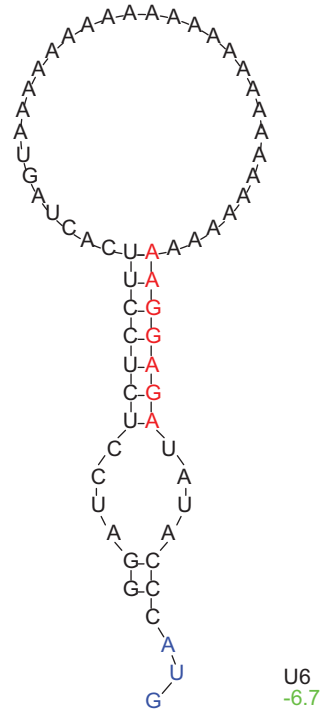

Figure 1.3 Synthetic RNA thermometer example (after Neupert *et al.*[94]).

see for example Figure 1.3, containing the ribosome-binding site can be produced.[93–95] Ideas for the use of the DNA backbone for temperature sensors and switches have also been explored.[12]

1.3 Selection

Conventionally, the selection of a specific sensor or system for temperature measurement involves consideration of a number of parameters including:

(1) Uncertainty;
(2) Temperature range;
(3) Thermal disturbance;
(4) Level of contact;
(5) Size of the sensor;
(6) Transient response;
(7) Sensor protection;
(8) Availability; and
(9) Cost.

In the case of nanoscale applications, however, the small scale and specific requirements, along with available technology may dictate the use of a

Table 1.1 Typical spatial resolution, temperature resolution and response times for a range of nanoscale-relevant temperature measurement methods.

Method	Spatial resolution/μm	Temperature resolution/K	Response time/μs
Infrared thermography	10	10^{-1}	10
Thermoreflectance	10^{-1}	10^{-2}	10^{-1}
Raman	1	10^{-1}	10^{6}
Thermocouple	10^{2}	10^{-1}	10
Fluorescence	10^{-1}	10^{-2}	10
Near-field scanning optical microscopy	10^{-2}	10^{-1}	10
Liquid crystals	10	10^{-1}	10^{2}
Scanning thermal microscopy	10^{-1}	10^{-1}	10^{2}
Transmission electron microscopy	10^{-2}	10^{-1}	10
Optical interferometry	1	10^{-5}	10^{-3}

particular method. Despite any apparent lack of choice, consideration still needs to be given to the uncertainty associated with the measurement. A common assumption is that because fundamental physics is being used, there is no need to consider a measurement uncertainty. However, reasonably simple analysis approaches can be used to evaluate the thermal disturbance associated with the incorporation of a probe into a medium of interest.[29] This may, depending on the application, involve just a conduction equation analysis accounting for any differences in thermal conductivity between the undisturbed medium, and that with the sensor embedded, or coating applied, or may involve a thermal radiation calculation to evaluate whether the presence of a probe has altered the thermal radiation exchanges significantly. It is all too easy to alter the temperature of a sample inadvertently due to the presence of an optical head. In addition, new methods such as the observation of Brownian motion or nanoparticles are emerging,[96] providing new opportunities and technology options to assess.

A summary of the approximate capabilities of a range of methods is given in Table 1.1. This has been adapted from the information given in ref. 26–28 and ref. 97.

In assessing the performance of a luminescent thermometer, a useful parameter is the relative sensitivity, defined by

$$S = \frac{\left(\frac{\partial Q}{\partial T}\right)}{Q} \tag{1.1}$$

Where Q, is an experimental parameter and corresponds to the quenching of luminescence with temperature. For example Brites *et al.*[98] determined a sensitivity of 4.9% K^{-1} for an orthosilicate/aminopropyltriethoxysilane (TEOS/APTES) organosilica shell co-doped with $[Eu(btfa)_3(MeOH)(bpeta)]$ and $[Tb(btfa)_3(MeOH)(bpeta)]$ β-diketonate chelates using the integrated areas I_{Eu} and I_{Tb} of the $^5D_0$–$^7F_2$ (I_{Eu} at 612 nm) and $^5D_4$–$^7F_5$ (I_{Tb} at 545 nm)

Table 1.2 Figure of merit sensitivity ($\%K^{-1}$) and temperature range (K) for a selection of luminescent molecular thermometers. Data adapted from Brites *et al.*[27]

Phosphor	S_m	ΔT (T_m)
Ru(phen)	2.5	280–325 (320)
Fluorescein D–Texas Red A in DNA	4.5	278–318 (295)
PtOEP	4.6	290–320 (305)
RhB in PDMS	2.3	293–373 (363)
C_{70} in PtBMA	2.2	293–363 (363)
PNIPAM	10.4	293–318 (308)
Mutant of lacI (Its265)	19.6	308–318 (318)
(CdSe)ZnS QDs	2.2	278–313 (313)
YAG:Ce nanoparticles	0.2	315–350 (350)
$Y_2O_3:Eu^{3+}$	2.6	473–973 (973)
$Eu(tta)_3 \cdot 3H_2O$ embedded in PMMA	4.4	293–333 (330)

transitions, in this case, $Q = I_{Eu}^2 - I_{Tb}^2$. Spatial and temporal resolutions of 0.42 μm and 4.8 ms, respectively, have been reported.[99]

Values for the sensitivity of a range of luminescent molecular thermometers are given in Table 1.2, adapted from Brites *et al.*[27]

1.4 Conclusions

The measurement of temperature at the nanoscale represents a practical reality with a wide range of techniques having been demonstrated. A particular challenge remains for systems where thermal gradients exist, the temperature is at cryogenic levels and the thermal mass is low, arising from the fundamental requirement for sufficient continuum to enable a meaningful definition of temperature for the system concerned. Analysis methods have been proposed to enable calculation of the necessary length scales for meaningful measurements of temperature, with the length scale dependent on the material properties and the temperature. The host of technologies available has now led to choice for some applications as well as bespoke solutions emerging, for example the measurement of temperature on microelements in circuitry and within cells. The development of understanding at the cellular level offers opportunities for the transfer of this knowledge to the design of new synthetic devices for both measurement and control. The pioneering work on nanoscale temperature measurement has certainly opened up insight across many domains, as well as posing some fundamental challenges both in terms of the technology and making sense of the data and its validity.

References

1. C. F. Chapman, Y. Liu, G. J. Sonek and B. J. Tromberg, The use of exogenous fluorescent probes for temperature measurements in single living cells, *Photochem. Photobiol.*, 1995, **62**, 416–425.

2. O. Zohar, M. Ikeda, H. Shinagawa, H. Inoue, H. Nakamura, D. Elbaum, D. L. Alkon and T. Yoshioka, Thermal imaging of receptor-activated heat production in single cells, *Biophys. J.*, 1998, **74**, 82–89.
3. M. Suzuki, V. Tseeb, K. Oyama and S. Ishiwata, Microscopic detection of thermogenesis in a single HeLa cell, *Biophys. J.*, 2007, **92**, L46–L48.
4. N. Mohan, C. S. Chen, H. H. Hsieh, Y. C. Wu and H. C. Chang, In vivo imaging and toxicity assessments of fluorescent nanodiamonds in Caenorhabditis elegans, *Nano Lett.*, 2010, **10**, 3692–3699.
5. C. Gota, K. Okabe, T. Funatsu, Y. Harada and S. Uchiyama, Hydrophilic fluorescent nanogel thermometer for intracellular thermometry, *J. Am. Chem. Soc.*, 2009, **131**, 2766–2767.
6. H. Huang, S. Delikanli, H. Zeng, D. M. Ferkey and A. Pralle, Remote control of ion channels and neurons through magnetic-field heating of nanoparticles, *Nat. Nanotechnol.*, 2010, **5**, 602–606.
7. J. M. Yang, H. Yang and L. W. Lin, Quantum dot nano thermometers reveal heterogeneous local thermogenesis in living cells, *ACS Nano*, 2011, **5**, 5067–5071.
8. K. Okabe, N. Inada, C. Gota, Y. Harada, T. Funatsu and S. Uchiyama, Intracellular temperature mapping with a fluorescent polymeric thermometer and fluorescence lifetime imaging microscopy, *Nat. Commun.*, 2012, **3**, 705.
9. C. L. Wang, R. Z. Xu, W. J. Tian, X. L. Jiang, Z. Y. Cui, M. Wang, H. M. Sun, K. Fang and N. Gu, Determining intracellular temperature at single-cell level by a novel thermocouple method, *Cell Res.*, 2011, **21**, 1517–1519.
10. P. Neumann, I. Jakobi, F. Dolde, C. Burk, R. Reuter, G. Waldherr, J. Honert, T. Wolf, A. Brunner, J. H. Shim, D. Suter, H. Sumiya, J. Isoya and J. Wrachtrup, High-precision nanoscale temperature sensing using single defects in diamond, *Nano Lett.*, 2013, **13**, 2738–2742.
11. G. Kucsko, P. C. Maurer, N. Y. Yao, M. Kubo, H. J. Noh, P. K. Lo, H. Park and M. D. Lukin, Nanometre-scale thermometry in a living cell, *Nature*, 2013, **500**, 54–58.
12. A. T. Jonstrup, J. Fredsoe and A. H. Andersen, DNA hairpins as temperature switches, thermometers and ionic detectors, *Sensors*, 2013, **13**, 5937–5944.
13. R. Schirhagl, K. Chang, M. Loretz and C. L. Degen, Nitrogen-vacancy centers in Diamond: nanoscale sensors for physics and biology, *Annu. Rev. Phys. Chem.*, 2014, **65**, 83–105.
14. P. Kolodner and J. A. Tyson, Remote thermal imaging with 0.7 mm spatial resolution using temperature-dependent fluorescent thin films, *Appl. Phys. Lett.*, 1983, **42**, 117–119.
15. L. Aigouy, G. Tessier, M. Mortier and B. Charlot, Scanning thermal imaging of microelectronic circuits with a fluorescent nanoprobe, *Appl. Phys. Lett.*, 2005, **87**(18), 184105.
16. G. Tessier, M. Bardoux, C. Boue and D. Fournier, Back side thermal imaging of integrated circuits at high spatial resolution, *Appl. Phys. Lett.*, 2007, **90**, 171112.

17. W. J. Liu and B. Z. Yang, Thermography techniques for integrated circuits and semiconductor devices, *Sens. Rev.*, 2007, **27**, 298–309.
18. W. Jung, Y. W. Kim, D. Yim and J. Y. Yoo, Microscale surface thermometry using SU8/Rhodamine-B thin layer, *Sens. Actuators, A*, 2011, **171**, 228–232.
19. H. B. Mao, T. L. Yang and P. S. Cremer, A microfluidic device with a linear temperature gradient for parallel and combinatorial measurements, *J. Am. Chem. Soc.*, 2002, **124**, 4432–4435.
20. R. Samy, T. Glawdel and C. L. Ren, Method for microfluidic whole-chip temperature measurement using thin-film poly(dimethylsiloxane)/rhodamine B, *Anal. Chem.*, 2008, **80**, 369–375.
21. C. Gosse, C. Bergaud and P. Low, Molecular probes for thermometry in microfluidic devices, in *Thermal Nanosystems and Nanomaterials, Topics in Advanced Physics*, ed. S. Volz, Springer-Verlag, Berlin, 2009, vol. 118, pp. 301–341.
22. T. Barilero, T. Le Saux, C. Gosse and L. Jullien, Fluorescent thermometers for dual-emission-wavelength measurements: molecular engineering and application to thermal imaging in a microsystem, *Anal. Chem.*, 2009, **81**, 7988–8000.
23. E. M. Graham, K. Iwai, S. Uchiyama, A. P. de Silva, S. W. Magennis and A. C. Jones, Quantitative mapping of aqueous microfluidic temperature with sub-degree resolution using fluorescence lifetime imaging microscopy, *Lab Chip*, 2010, **10**, 1267–1273.
24. J. Feng, K. J. Tian, D. H. Hu, S. Q. Wang, S. Y. Li, Y. Zeng, Y. Li and G. Q. Yang, A Triarylboron-based fluorescent thermometer: sensitive over a wide temperature range, *Angew. Chem., Int. Ed.*, 2011, **50**, 8072–8076.
25. C. Y. Wang and L. J. Chen, Nanothermometers for transmission electron microscopy – fabrication and characterization, *Eur. J. Inorg. Chem.*, 2010, 4298–4303.
26. J. Christofferson, K. Maize, Y. Ezzahri, J. Shabani, X. Wang and A. Shakouri, Microscale and nanoscale thermal characterization techniques, *J. Electron. Packag.*, 2008, **130**, 041101–041106.
27. C. D. S. Brites, P. P. Lima, N. J. O. Silva, A. Millan, V. S. Amaral, F. Palacio and L. D. Carlos, Thermometry at the nanoscale, *Nanoscale*, 2012, **4**, 4799–4829.
28. P. R. N. Childs, J. R. Greenwood and C. A. Long, Review of Temperature measurement, *Rev. Sci. Instrum.*, 2000, **71**, 2959–2978.
29. P. R. N. Childs, *Practical Temperature Measurement*, Butterworth Heinemann, 2001.
30. J. V. Nicholas and D. R. White *Traceable Temperatures*, Wiley, 1994.
31. Temperature, ed. C. M. Herzfield, *Its Measurement and Control in Science and Industry*, Rheinhold, 1962, vol. 3.
32. Temperature, ed. H. H. Plumb, *Its Measurement and Control in Science and Industry*, American Institute of Physics, 1972, vol. 4.
33. Temperature, ed. J. F. Schooley, *Its Measurement and Control in Science and Industry*, American Institute of Physics, 1992, vol. 6.

34. Temperature, ed. J. F. Schooley, *Its Measurement and Control in Science and Industry*, American Institute of Physics, 1982, vol. 5.
35. Temperature, ed. D. C. Ripple, *Its Measurement and Control in Science and Industry*, American Institute of Physics, 2002, vol. 7.
36. Temperature, ed. C. W. Meyer, *Its Measurement and Control in Science and Industry*, American Institute of Physics, 2012, vol. 8.
37. J. B. Weaver, Bioimaging: Hot nanoparticles light up cancer, *Nat. Nanotechnol.*, 2010, **5**, 630–631.
38. K. M. McCabe and M. Hernandez, Molecular thermometry, *Pediatr. Res.*, 2010, **67**, 469–475.
39. M. J. Hartmann, Minimal length scales for the existence of local temperature, *Contemp. Phys.*, 2006, **47**(2), 89–102.
40. H. J. Kreuzer, *Nonequilibrium Thermodynamics and its Statistical Foundation*, Clarandon Press, Oxford, 1981.
41. B. W. Mangum and G. T. Furukawa, Guidelines for realizing the ITS-90, NIST Tech, note 1265, 1990.
42. M. Alaskar, M. Ames, C. Liu, S. Connor, R. Horne, K. Li and Y. Cui, Smart nanosensors for in-situ temperature measurement in fractured geothermal reservoirs, Australian Geothermal Energy Conference, 2011.
43. C. Meola and G. M. Carlomagno, Recent advances in the use of infrared thermography, *Meas. Sci.Technol.*, 2004, **15**, R27–R58.
44. S. H. Kim, J. Noh, M. K. Jeon, K. W. Kim, L. P. Lee and S. I. Woo, Micro-Raman thermometry for measuring the temperature distribution inside the microchannel of a polymerase chain reaction chip, *J. Micromech. Microeng.*, 2006, **16**, 526–530.
45. Y. Yue, G. Eres, X. Wang and L. Guo, Characterization of thermal transport in micro/nanoscale wires by steady-state electro-Raman-thermal technique, *Appl. Phys. A: Mater. Sci. Process.*, 2009, **97**, 19–23.
46. O. Frazão, C. Correia, J. L. Santos and J. M. Baptista, Raman fibre Bragg-grating laser sensor with cooperative Rayleigh scattering for strain-temperature measurement, *Meas. Sci. Technol.*, 2009, **20**, 045203.
47. T. Beechem, S. Graham, S. P. Kearney, L. M. Phinney and J. R. Serrano, Simultaneous mapping of temperature and stress in microdevices using micro-Raman spectroscopy, *Rev. Sci. Instrum.*, 2007, **78**.
48. L. Song, W. Ma, Y. Ren, W. Zhou, S. Xie, P. Tan and L. Sun, Temperature dependence of Raman spectra in single-walled carbon nanotube rings, *Appl. Phys. Lett.*, 2008, **9**.
49. S. Piscanec, M. Cantoro, A. C. Ferrari, J. A. Zapien, Y. Lifshitz, S. T. Lee, S. Hofmann and J. Robertson, Raman spectroscopy of silicon nanowires, *Phys. Rev. B: Condens. Matter Mater. Phys.*, 2003, **68**.
50. I. Calizo, A. A. Balandin, W. Bao, F. Miao and C. N. Lau, Temperature dependence of the Raman spectra of graphene and graphene multilayers, *Nano Lett.*, 2007, **7**, 2645–2649.
51. M. E. Kose, B. F. Carroll and K. S. Schanze, Preparation and spectroscopic properties of a dual luminophore pressure sensitive paint, *Langmuir*, 2005b, **21**, 9121–9129.

52. M. E. Kose, A. Omar, C. A. Virgin, B. F. Carroll and K. S. Schanze, Principal component analysis calibration method for dual luminophore pressure sensitive paints, *Langmuir*, 2005b, **21**, 9110–9120.
53. N. Chandrasekharan and L. A. Kelly, A dual fluorescence temperature sensor based on perylene/exciplex interconversion, *J. Am. Chem. Soc.*, 2001, **123**, 9898–9899.
54. G. Walker, V. Sundar, C. Rudzinski, A. Wun, M. Bawendi and D. Nocera, Quantum-dot optical temperature probes, *Appl. Phys. Lett.*, 2003, **83**, 3555–3557.
55. H. Sakaue, A. Aikawa, Y. Iijima, T. Kuriki and T. Miyazaki, Quantum dots as global temperature measurements, in *Quantum Dots – A Variety of New Applications*, ed. A. Al-Ahmadi, InTech ch. 7, 2012.
56. W. G. J. H. M. van Sark, P. L. T. M. Frederix, A. A. Bol, H. C. Gerritsen and A. Meijerink, Blueing, bleaching, and blinking of single CdSe/ZnS quantum dots, *Chem. Phys. Chem.*, 2002, **3**, 871–879.
57. K. H. Isnaeni Kim, D. L. Nguyen, H. Lim, T. N. Pham and Y. H. Cho, Shell layer dependence of photoblinking in CdSe/ZnSe/ZnS quantum dots, *Appl. Phys. Lett.*, 2011, **98**, 012109–012112.
58. M. Nakamura, S. Ozaki, M. Abe, T. Matsumoto and K. Ishimura, One-pot synthesis and characterization of dual fluorescent thiol-organosilica nanoparticles as non-photoblinking quantum dots and their applications for biological imaging, *J. Mater. Chem.*, 2011, **21**, 4689–4695.
59. M. J. Holmes, K. Choi, S. Kako, M. Arita and Y. Arakawa, Room-temperature triggered single photon emission from a III-nitride site-controlled nanowire quantum dot, *Nano Lett.*, 2014, **14**(2), 982–986.
60. B. Somogyi and A. Gali, Computational design of in vivo biomarkers, *J. Phys.: Condens. Matter*, 2014, **26**, 143202.
61. A. L. Heyes, Thermographic phosphor thermometry for gas turbines, in *Advanced Measurement Techniques for Aero and Stationary Gas Turbines*, ed. C. H. Sieverding and J. F. Brouckaert, VKI LS 2004-04, 2004.
62. A. L. Heyes, On the design of phosphors for high temperature thermometry, *J. Lumin.*, 2009, **129**, 2004–2009.
63. Y. Cui, W. Zou, R. Song, J. Yu, W. Zhang, Y. Yang and G. Qian, A ratiometric and colorimetric luminescent thermometer over a wide temperature range based on a lanthanide coordination polymer, *Chem. Commun.*, 2014, **50**, 719–721.
64. W. Li, Z. J. Coppens, D. Greg Walker and J. G. Valentine, Electron beam physical vapor deposition of thin ruby films for remote temperature sensing, *J. Appl. Phys.*, 2013, **113**, 163509.
65. V. Lojpur, M. G. Nikolic, D. Jovanovic, M. Medic, Z. Antic and M. D. Dramicanin, Luminescence thermometry with Zn_2SiO_4:Mn^{2+} powder, *Appl. Phys. Lett.*, 2013, **103**, 141912.
66. L. Liu, S. Creten, Y. Firdaus, J. Jesus, A. Flores Cuautle, M. Kouyate, M. Van der Auweraer and C. Glorieux, Fluorescence spectra shape based dynamic thermometry, *Appl. Phys. Lett.*, 2014, **104**, 031902.

67. O. Yarimaga, S. Lee, D. Y. Ham, J. M. Choi, S. G. Kwon, M. Im, S. Kim, J.-M. Kim and Y.-K. Choi, Thermofluorescent conjugated polymer sensors for nano- and microscale temperature monitoring, *Macromol. Chem. Phys.*, 2011, **212**, 1211–1220.
68. F. Vetrone, R. Naccache, A. Zamarron, A. J. De La Fuente, F. Sanz-Rodriguez, L. M. Maestro, E. M. Rodriguez, D. Jaque and J. Garcia, Temperature sensing using fluorescent nanothermometers, *ACS Nano*, 2010, **4**, 3254–3258.
69. C. Paviolo, A. H. A. Clayton, S. L. McArthur and P. R. Stoddart, Temperature measurement in the microscopic regime: a comparison between fluorescence lifetime- and intensity-based methods, *J. Microsc.*, 2013, **250**, 179–188.
70. Q. Fu, G. V. R. Rao, L. K. Ista, Y. Wu, B. P. Andrzejewski, L. A. Sklar, T. L. Ward and G. P. Lopez, Control of molecular transport through stimuli-responsive ordered mesoporous materials, *Adv. Mater.*, 2003, **15**, 1262–1266.
71. A. Schlossbauer, S. Warncke, P. M. E. Gramlich, J. Kecht, A. Manetto, T. Carell and T. Bein, A Programmable DNA-Based Molecular Valve for Colloidal Mesoporous Silica, *Angew. Chem., Int. Ed.*, 2010, **49**, 4734–4737.
72. E. Aznar, L. Mondragon, J. V. Ros-Lis, F. Sancenon, M. D. Marcos, R. Martinez-Manez, J. Soto, E. Perez-Paya and P. Amoros, Finely tuned temperature-controlled cargo release using paraffin-capped mesoporous silica nanoparticles, *Angew. Chem., Int. Ed.*, 2011, **50**, 11172–11175.
73. P. Bon, N. Belaid, D. Lagrange, C. Bergaud, H. Rigneault, S. Monneret and G. Baffou, Three-dimensional temperature imaging around a gold microwire, *Appl. Phys. Lett.*, 2013, **102**, 244103.
74. G. Binnig, H. Rohrer, C. Gerber and E. Weibel, Tunneling through a controllable vacuum gap, *Appl. Phys. Lett.*, 1982, **40**, 178–180.
75. A. Majumdar, J. P. Carrejo and J. Lai, Thermal imaging using the atomic force microscope, *Appl. Phys. Lett.*, 1993, **62**, 2501–2503.
76. G. Mills, H. Zhou, A. Midha, L. Donaldson and J. M. R. Weaver, Scanning thermal microscopy using batch fabricated thermocouple probes, *Appl. Phys. Lett.*, 1998, **72**, 2900–2902.
77. A. Hammiche, M. Reading, H. M. Pollock, M. Song and D. J. Hourston, Localized thermal analysis using a miniaturized resistive probe, *Rev. Sci. Instrum.*, 1996, **67**, 4268–4274.
78. P. G. Royall, V. L. Kett, C. S. Andrews and D. Q. M. Craig, Identification of crystalline and amorphous regions in low molecular weight materials using microthermal analysis, *J. Phys. Chem. B*, 2001, **105**, 7021–7026.
79. S. Lefevre and S. Volz, 3ω-scanning thermal microscope, *Rev. Sci. Instrum.*, 2005, **76**, 033701.
80. J. R. Greenwood, P. R. N. Childs and P. Chaloner, Gold leads to PRTs for monitoring high temperatures, *Gold Bull.*, 1999, **32**(3), 85–89.
81. *US Pat.*, No. 6905736, Fabrication of nano-scale temperature sensors and heaters, 2005.

82. D. C. Chu, W. K. Wong, K. E. Goodson and R. F. W. Pease, Transient temperature measurements of resist heating using nanothermocouples, *J. Vac. Sci. Technol., B*, 2003, **21**, 2985–2989.
83. Y. H. Gao and Y. Bando, Carbon nanothermometer containing gallium, *Nature*, 2002, **415**, 599.
84. C. Y. Wang, N. W. Gong and L. J. Chen, High sensitivity solid state Pb(core)/ZnO(shell) nanothermometers fabricated with a facile galvanic displacement method, *Adv. Mater.*, 2008, **20**, 4789–4792.
85. N. W. Gong, M. Y. Lu, C. Y. Wang, Y. Chen and L. J. Chen, Au(Si)-filled Beta-Ga_2O_3nanotubes as wide range high temperature nanothermometers, *Appl. Phys. Lett.*, 2008, **92**, 073101–073103.
86. Y. B. Li, Y. Bando and D. Golberg, Single-crystalline In_2O_3 nanotubes filled with In, *Adv. Mater.*, 2003, **15**, 581–585.
87. P. D. Tovee, M. E. Pumarol, M. C. Rosamond, R. Jones, M. C. Petty, D. A. Zezeb and O. V. Kolosov, Nanoscale resolution scanning thermal microscopy using carbon nanotube tipped thermal probes, *Phys.Chem.Chem.Phys.*, 2014, **16**, 1174–1181.
88. B. Klinkert and F. Narberhaus, Microbial thermosensors, *Cell. Mol. Life Sci.*, 2009, **66**, 2661–2676.
89. D. Albanesi, M. Martin, F. Trajtenberg, M. C. Mansilla, A. Haouz, P. M. Alzari, D. de Mendoza and A. Buschiazzo, Structural plasticity and catalysis regulation of a thermosensor histidine kinase, *Proc. Natl. Acad. Sci. U. S. A.*, 2009, **106**, 16185–16190.
90. J. Kortmann, S. Sczodrok, J. Rinnenthal, H. Schwalbe and F. Narberhaus, Translation on demand by a simple RNA-based thermosensor, *Nucleic Acids Res.*, 2011, **39**, 2855–2868.
91. S. Chowdhury, C. Maris, F. H. T. Allain and F. Narberhaus, Molecular basis for temperature sensing by an RNA thermometer, *EMBO J.*, 2006, **25**, 2487–2497.
92. F. Narberhaus, T. Waldminighaus and S. Chowdhury, RNA thermometers, *FEMS Microbiol. Rev.*, 2006, **30**, 3–16.
93. T. Waldminghaus, J. Kortmann, S. Gesing and F. Narberhaus, Generation of synthetic RNA-based thermosensors, *Biol. Chem.*, 2008, **389**, 1319–1326.
94. J. Neupert, D. Karcher and R. Bock, Design of simple synthetic RNA thermometers for temperature-controlled gene expression in Escherichia coli, *Nucleic Acids Res.*, 2008, **36**, e124.
95. J. Neupert and R. Bock, Designing and using synthetic RNA thermometers for temperature-controlled gene expression in bacteria, *Nat. Protocol*, 2009, **4**, 1262–1273.
96. J. Millen, T. Deesuwan, P. Barker and J. Anders, Nanoscale temperature measurements using non-equilibrium Brownian dynamics of a levitated nanosphere, *Nat. Nanotechnol.*, 2014.
97. M. Asheghi and Y. Yang Micro- and nano-scale diagnostic techniques for thermometry and thermal imaging of microelectronic and data storage

devices, in *Microscale Diagnostic Techniques*, ed. K. S. Breuer, Springer-Verlag, 2005, pp. 155–196.

98. C. D. S. Brites, P. P. Lima, N. J. O. Silva, A. Millan, V. S. Amaral, F. Palacio and L. D. Carlos, Thermometry at the nanoscale using lanthanide-containing organic–inorganic hybrid materials, *J. Lumin.*, 2013a, **133**, 230–232.
99. C. D. S. Brites, P. P. Lima, N. J. O. Silva, A. Millan, V. S. Amaral, F. Palacio and L. D. Carlos, Organic-Inorganic Eu^{3+}/Tb^{3+} codoped hybrid films for temperature mapping in integrated circuits, *Front. Chem.*, 2013b, **1**, 9.